JOURNAL OF ENVIRONMENTAL SCIENCES 95 (2020) 155–164

Available online at www.sciencedirect.com

ScienceDirect

www.elsevier.com/locate/jes

JES JOURNAL OF ENVIRONMENTAL SCIENCES

www.jesc.ac.cn

Reactive uptake of NO_2 on volcanic particles: A possible source of HONO in the atmosphere

Manolis N. Romanias[1,*], *Yangang Ren*[2], *Benoit Grosselin*[2], *Véronique Daële*[2], *Abdelwahid Mellouki*[2], *Pavla Dagsson-Waldhauserova*[3,4], *Frederic Thevenet*[1]

[1] *IMT Lille Douai, Univ. Lille, SAGE, F-59000 Lille, France*
[2] *CNRS-ICARE/OSUC, 45071 Orléans, France*
[3] *Agricultural University of Iceland, Keldnaholt, Reykjavik 112, Iceland*
[4] *Faculty of Environmental Sciences, Czech University of Life Sciences, Prague 165 21, Czech Republic*

ARTICLE INFO

Article history:
Received 14 September 2019
Revised 28 November 2019
Accepted 17 March 2020
Available online 4 May 2020

Keywords:
Volcanic dust
HONO
Uptake coefficients
Product yields
Simulated atmospheric conditions

ABSTRACT

The heterogeneous degradation of nitrogen dioxide (NO_2) on five samples of natural Icelandic volcanic particles has been investigated. Laboratory experiments were carried out under simulated atmospheric conditions using a coated wall flow tube (CWFT). The CWFT reactor was coupled to a blue light nitrogen oxides analyzer (NO_x analyzer), and a long path absorption photometer (LOPAP) to monitor in real time the concentrations of NO_2, NO and HONO, respectively. Under dark and ambient relative humidity conditions, the steady state uptake coefficients of NO_2 varied significantly between the volcanic samples probably due to differences in magma composition and morphological variation related with the density of surface OH groups. The irradiation of the surface with simulated sunlight enhanced the uptake coefficients by a factor of three indicating that photo-induced processes on the surface of the dust occur. Furthermore, the product yields of NO and HONO were determined under both dark and simulated sunlight conditions. The relative humidity was found to influence the distribution of gaseous products, promoting the formation of gaseous HONO. A detailed reaction mechanism is proposed that supports our experimental observations. Regarding the atmospheric implications, our results suggest that the NO_2 degradation on volcanic particles and the corresponding formation of HONO is expected to be significant during volcanic dust storms or after a volcanic eruption.

Introduction

Nitrogen dioxide (NO_2) is an important atmospheric pollutant that contributes to the formation of photochemical smog (von Schneidemesser et al., 2015). NO_2 acts as an intermediate species in several gas phase photochemical cycles occurring in the troposphere affecting the radical budgets for hydroperoxyl radicals (HO_x) and peroxy radicals (RO_x), as well as that of ozone (O_3). In addition, the chemistry of NO_2 is involved in the formation of organic nitrates (Nault et al., 2016; Perring et al., 2013; von Schneidemesser et al., 2015). Besides gas phase chemistry, the heterogeneous reactivity of NO_2 with atmospheric particles has been shown to play an important role in atmospheric processes. NO_2 reacts with aerosols forming nitrous acid (HONO), a key atmospheric species, precursor of the major atmospheric oxidant: OH radicals (Mellouki

* Corresponding author.
E-mail: emmanouil.romanias@imt-lille-douai.fr (M.N. Romanias).

https://doi.org/10.1016/j.jes.2020.03.042
1001-0742/

et al., 2015). So far, atmospheric simulation models fail to reproduce the unexpectedly high daytime concentrations of HONO reported in field campaigns, suggesting the existence of new, yet unknown, sources of HONO (Kleffmann, 2007; Romer et al., 2018). Therefore, it has been suggested that the heterogeneous conversion of NO_2 to HONO could possibly explain the discrepancies between atmospheric models and field observations (Romer et al., 2018).

The heterogeneous reaction of NO_2 on various type of atmospheric particles, e.g., salts, soot, mineral dust and proxies, has been already reported in literature (Crowley et al., 2010; George et al., 2015; Tang et al., 2017). However, the interaction of NO_2 with volcanic particles under simulated atmospheric conditions has not been studied. Actually, the role of volcanic aerosols on tropospheric chemistry has not been thoroughly evaluated yet. Volcanic aerosols may act as platforms for the scavenging or conversion of key atmospheric species (e.g., NO_2, O_3, SO_2 etc.), and thus, impact the tropospheric oxidation capacity regionally, or in a larger scale such as during massive volcanic eruptions or during extreme dust storms of volcanic dust as reported for instance in Iceland (Arnalds et al., 2016; Arnalds et al., 2013; Moroni et al., 2018; Ovadnevaite et al., 2009).

Considering that nearly 10% of the world population is living in the vicinity of active volcanos (Auker et al., 2013), it is expected that pollutants emitted from anthropogenic sources, such as nitrogen oxide species (NO_x), O_3 etc. can interact or react with naturally emitted volcanic gases or volcanic aerosols. A prime example is Mexico City, known as one of the most polluted city in the world, situated 70 km away from the frequently erupting Popocatépetl volcano. Besides, distal urban environments can also be impacted by volcanic pollution. Resuspension of volcanic ash, defined as volcanic dust, or v-dust, for the following of the paper, can prolong the effects of volcanic eruptions several months after the eruption is finished (Arnalds et al., 2013; Butwin et al., 2019; Wilson et al., 2011). The recent eruptions of Icelandic volcanoes Eyjafjallajökull in 2010 and Grimsvötn in 2011, resulted in the dispersal of massive loads of ashes and aerosols over a large part of Europe and Northern Atlantic (Gudmundsson et al., 2012; Ilyinskaya et al., 2017). Holuhraun (2014–2015) was an effusive eruption occurring in the center of volcanic dust hot spot, but volcanic dust was frequently suspended during the eruption (Pfeffer et al., 2018; Vignelles et al., 2016). Therefore, volcanic aerosols are regularly emitted in the atmosphere and recent studies have shown that their lifetime is significantly longer than it has been estimated (Boichu et al., 2016).

Consequently, the objective of the current study is to determine experimentally how efficiently NO_2 is scavenged on volcanic particles and to evaluate whether this interaction can be a significant source of HONO in the atmosphere - on local or regional scale - during severe volcanic dust storms or volcanic eruptions. To that end, laboratory experiments have been carried out under simulated atmospheric conditions (temperature, relative humidity, NO_2 concentrations and simulated sunlight radiation) employing a flow tube coupled with state of the art instrumentation for the simultaneous detection of NO_2, NO and HONO. The reactive uptake coefficients of NO_2 are measured and the yields of the products formed, and the mechanism of the reaction are addressed.

1. Materials and methods

1.1. Materials

1.1.1. Origin of the volcanic samples

In the current paper, Iceland was chosen as a case study. Iceland is a very active geological site of Earth with more than 30 active volcanoes and large eruptions occurring every 3–5 years. Hence it is considered as the largest volcanic desert on Earth (Arnalds et al., 2016) with estimated dust deposition of 31–40 million tons per year (Arnalds et al., 2014), that could represents up to 7% of total global dust emissions and up to 21% of the Saharan dust emissions (Arnalds et al., 2014; Engelstaedter et al., 2006). Remote sensing studies have evidenced that volcanic plumes formed after a volcanic eruption in Iceland can travel thousands of kilometers impacting urban populated areas of northern Europe (Boichu et al., 2016). Moreover, Iceland is one of the most active aeolian areas on the planet, where unstable sandy surfaces are widespread and are subjected to frequent high-velocity winds, resulting in numerous wind erosion events and massive volcanic dust storms (Arnalds et al., 2016). In Iceland, around 100 dust events are reported each year (Arnalds et al., 2014); up to 300,000 tons of dust can be emitted in a single storm. Particulate matter 10 μm or less in diameter (i.e., PM_{10}) mass concentrations during dust storms can exceed 7000 $\mu g/m^3$ with a 1000 $\mu g/m^3$ 24-hr average concentration (Dagsson-Waldhauserova et al., 2015; Thorsteinsson et al., 2011) striking populated areas such as Reykjavik (Dagsson-Waldhauserova et al., 2016). Satellite images confirm that during a dust storm, v-dust particles can travel distances longer than 1000 km impacting the air quality of central Greenland and northern Europe (Arnalds et al., 2016). In a recent study (Đorđević et al., 2019) it has been shown that volcanic dust from Iceland can be transported to even central Balkans, and authors pointed at the fact that Icelandic dust can contribute to impaired air quality in mainland Europe. Icelandic dust is also transported towards Arctic (Groot Zwaaftink et al., 2017; Moroni et al., 2018).

The volcanic samples investigated in the present work were collected from different desert regions of Iceland, so called dust hot spots Hagavatn, Mýrdalssandur, Maelifellssandur and Dyngjusandur, while the fifth sample of Eyjafjallajökull volcanic ash, named typical ash in the following of the article, was collected several hours after the eruption of the Eyjafjallajökull in 2010 (Gislason et al., 2011). Details about the characterization of the physical and chemical properties of the samples can be found elsewhere (Baratoux et al., 2011; Dagsson-Waldhauserova et al., 2014b; Moroni et al., 2018; Urupina et al., 2019) and for clarity are briefly discussed in Appendix A. Supplementary data.

1.1.2. Gases

The laboratory experiments were carried out using dry zero air as bath gas (moisture level ca. 2 ppmV) inside a photochemical flow tube. For experiments requiring humid air, an extra flow of zero air passing through a bubbler containing ultrapure water (milli-Q, resistivity 18.2 MΩ·cm) was mixed with the dry air flow, in proportions required to reach the targeted relative humidity (RH). The exact RH in the gas flow is determined and monitored using a temperature and RH probe (KIMO HQ 210, KIMO instruments, UK). Certified gas cylinders were used as NO_2 source. For low concentration experiments, aiming to determine uptake coefficients in the flow tube, a NO_2 cylinder of 200 ppbV in air (Air Liquide, France) was used. As far as concerns the experiments carried out to determine the irradiance intensity inside the flow tube reactor, rather high concentrations of NO_2 were used supplied from a NO_2 cylinder of 50 ppmV in N_2 (Praxair, Belgium).

1.1.3. Surface preparation

A few mg of the volcanic sample was placed inside a Pyrex tube (20 cm length, 0.98 cm internal diameter) and, depending on the volcanic sample mass, diluted in 0.5–2 mL of water. Then the tube was hand-shaken, so that the water/dust suspension homogeneously spreads on the walls of the tube without any trace of the suspension to be removed after the

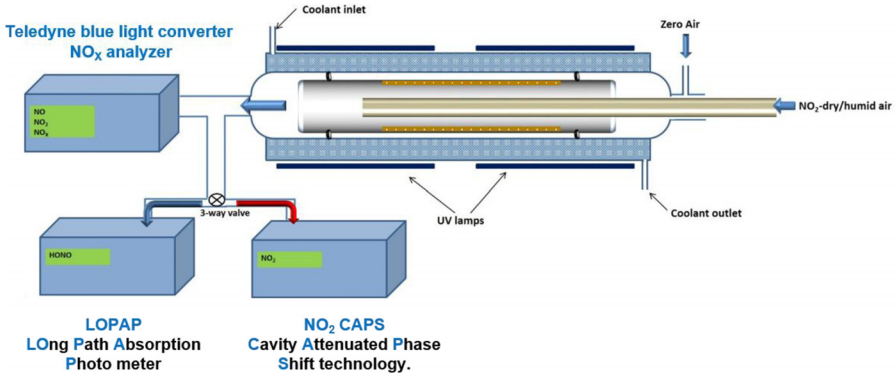

Fig. 1 – Schematic representation of the coated-wall flow-tube (CWFT) reactor used in this study. The space filled with the coolant in between the two walls is shaded in blue. The volcanic sample coating the inner surface of the Pyrex tube is shown in gray. The gas phase was monitored in real time with a nitrogen oxide (NO_x) analyzer, a long path absorption photometer (LOPAP) and occasionally with a cavity attenuated phase shift (CAPS) NO_2 analyzer. UV: ultraviolet.

deposition. Thereafter, the tube was heated at 120°C with a heat-gun for several minutes and further dried overnight in an oven at 100°C. It should be noted that potential modifications of the volcanic dust upon its dissolution in water in the process of slurry preparation and subsequent drying process are expected to be of limited extend (Urupina et al., 2019), and not to influence the uptake coefficients measured in the current study.

1.2. *Experimental set up*

The uptake experiments of NO_2 on the volcanic samples were performed using a horizontal double wall Pyrex atmospheric pressure coated wall flow tube reactor (CWFT) (Fig. 1). Further details of the experimental set up have been described in previous publications (Lasne et al., 2018; Urupina et al., 2019). The Pyrex tube with the inner coated surface was introduced into the main reactor along its axis. Two Viton O-rings were placed in both ends of the Pyrex tube to set its position. NO_2 was introduced in the reactor by means of a movable injector with internal diameter 0.3 cm. The injector can be moved along the main axis of the coated Pyrex tube, allowing the variation of the v-dust sample length exposed to NO_2 and consequently the contact time (t). The total flow rate was regulated between 200 and 400 mL/min, ensuring laminar flow conditions (Reynold number (Re) < 140).

The outlet gas flow was then mixed with a dry zero air flow (to compensate the sampling flow of the analytical instruments) and was either sent to a NO_x analyzer (Teledyne T 200UP, Teledyne API, USA) equipped with a blue light converter for the detection of NO_2 (detection limit 50 pptV), and nitrogen oxide (NO that appeared as reaction product), or to a long path absorption photometer (LOPAP, QUMA, Germany) to monitor HONO (reaction product) with a limit of detection of 1–2 pptV. Teledyne T 200UP NO_x analyzer uses photolysis in its conversion process; the gas flow passes through a conversion chamber and it is exposed to a blue light from two high powered ultraviolet light emitting diodes (LEDs) characterized by narrow emission bands centered at 395 nm as reported in Fig. 2 (bell curve area). The emission band of the LED includes NO_2 absorption band with negligible interferences expected from other gases such as HONO or NO_3 radicals. Consequently, unlike NO_x analyzers relying molybdenum converters, the selective detection of NO_2 is achieved. Based on the LED output intensity and wavelength range as well as the absorption cross section of HONO given in Fig. 2, we estimated that the HONO interference to NO_2 concentration to be lower than 3%.

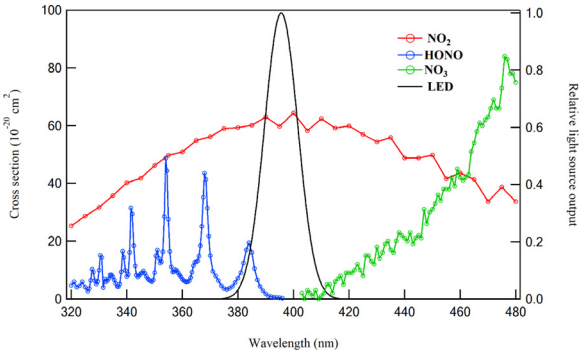

Fig. 2 – Absorption spectra of NO_2 and possible interferences (HONO, NO_3) along with the spectral output of the light-emitting diode (LED) centered at 395 nm.

To further evaluate possible interferences to NO_2 concentration measured along the uptake experiments, in a dedicated set of experiments a cavity attenuated phase shift (CAPS) NO_2 analyzer (AS32M, ENVEA S.A, France) was additionally coupled with the reactor. The NO_2 CAPS (detection limit 100 pptV) provides a direct absorption measurement of nitrogen dioxide at 450 nm and does not require any conversion of NO_2 to another species. Thus, no interference from other N-containing species are possible. Therefore, comparing the concentrations of NO_2 monitored with the NO_x analyzer and the CAPS we concluded that the possible interference of HONO is around 2% and, thus, included in our experimental uncertainties.

1.3. *Light source characterization*

The CWFT reactor was surrounded by 3 ultraviolet A lamps (UVA, Philips lighting 18 Watt; 315–400 nm with maximum emission at 352 nm) (Romanias et al., 2017). In order to characterize the irradiance intensity in the flow tube, the NO_2 photolysis frequency was measured as a function of the number of lamps turned on. These experiments were carried out with rather high NO_2 concentrations of ca. 10^{15} molecule/cm^3, i.e., 50 ppmV, using dry N_2 as bath gas. NO_2 concentration was monitored with a chemical ionization mass spectrometer (SIFT-MS, Syft Technology, New Zealand) (Romanías et al., 2016; Romanias et al., 2016; Zeineddine et al., 2017). The values of NO_2 photolysis frequency (J_{NO2} (sec^{-1}))

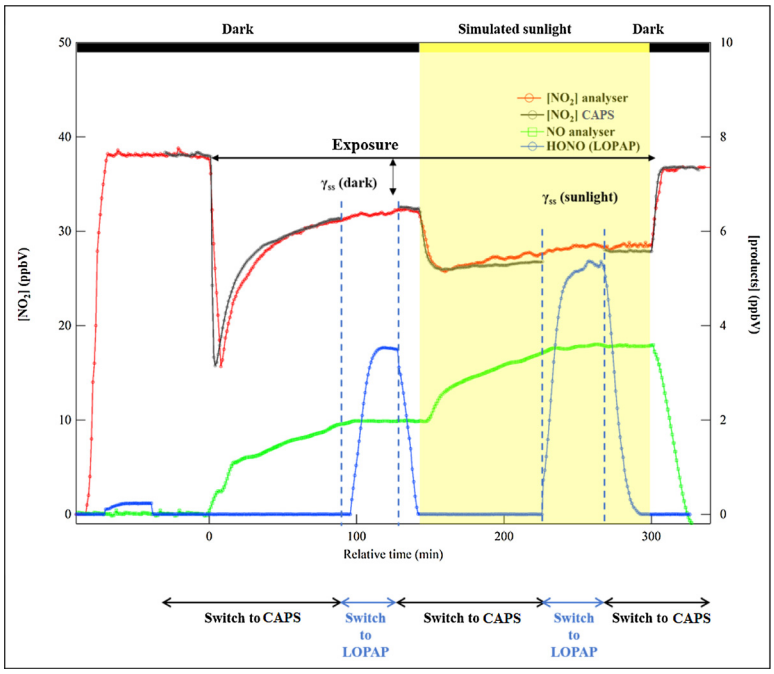

Fig. 3 – Typical experiment of NO_2 adsorption/reaction on Hagavatn volcanic sample where all instruments were coupled with the flow tube reactor. Left vertical axis corresponds to the concentration profile of NO_2, [NO_2]. The concentrations profiles of NO and HONO, denoted as [NO] and [HONO], respectively, are also displayed (right vertical axis). γ_{ss}(dark) and γ_{ss}(sunlight) refer to the data averaged to determine the uptake coefficients under dark and simulated sunlight conditions, respectively.

determined from the exponential decays of NO_2 for different numbers of lamps switched on were in the range of 4×10^{-3} – 15×10^{-3} sec^{-1} (Appendix A Fig. S2). Thus, it overlaps with the values of J_{NO2} measured in the atmosphere from cloudy to clear sky conditions (Barnard et al., 2004; Bohn et al., 2005; Topaloglou et al., 2005). Further information regarding the light source characterization experiments are reported in Appendix A. Supplementary data.

It has to be noted that under the experimental conditions where the uptake experiments were carried out, the gas phase loss of NO_2 due to its photodissociation is negligible. Indeed, for only 1 UV lamp, i.e., $J_{NO2} = 4.5 \times 10^{-3}$ sec^{-1}, denoted as simulated sunlight conditions in the following of the article, and with a residence time of 2 sec, the gas phase loss of NO_2 due to its photolysis was lower than 0.8%. In case more than one UV lamp was used, the flow in the reactor was increased to maintain gas phase consumption due to photolysis below 1.5% to avoid any impact on the measured uptake coefficient values. To conclude, our experimental measurements of the uptake coefficients and the product yields discussed below are not expected to be biased from interferences or experimental artifacts.

1.4. *Uptake of NO_2 on volcanic samples*

1.4.1. *Experimental procedure*

A typical uptake profile of NO_2 on Hagavatn sample under 30% of RH and 293 K is presented in Fig. 3. It was selected to present breakthrough profiles with all instruments coupled with the flow tube to analyze the outlet flow. In these experiments, the gas phase was continuously monitored with the NO_x analyzer, while either the NO_2 CAPS or the LOPAP were coupled to the flow tube (Fig. 3). First, the injector is placed at the downstream position of the reactor, ensuring no contact of the gas flow with the v-dust coating. At this stage the background concentration levels for all instruments is recorded. Afterwards, NO_2 is introduced in the reactor and a steady state concentration is achieved within a few minutes. The NO levels are close to zero while a very low formation of HONO was observed, probably due to hydrolysis of NO_2 on the wet Teflon lines (Finlayson-Pitts et al., 2003). This contribution was taken into account for further calculations of the product yields. Thereafter, the LOPAP was bypassed and the gas stream was driven through the NO_2 CAPS; as displayed in Fig. 3, the NO_2 concentrations measured with the analyzer and the CAPS are in excellent agreement. Subsequently, the injector is pulled out ($t = 0$ in Fig. 3) and the whole dust coating is exposed to the gas flow. A fast consumption of NO_2 was observed due to NO_2 uptake on the volcanic sample, and a gradual recovery to higher outlet concentrations was noticed. Simultaneously, NO was formed as a product of the heterogeneous reaction. After achieving a steady state consumption of NO_2 and formation of NO, the CAPS was bypassed to monitor the concomitant concentration of HONO with the LOPAP for ca. 25 min. Then, the flow was sent back to the CAPS. The next step in the experimental protocol was the irradiation of the surface with simulated sunlight; the initiated photo-induced processes on the surface of the volcanic particles lead to an extra consumption of NO_2 and an additional formation of NO. During the sample irradiation, the gas flow was sent to the LOPAP to determine the HONO concentrations formed and then switched back to the CAPS. In the last step, the injector is pushed back in, to control the NO_2 level. The steady state consumption of NO_2 and the formation products such as NO and HONO under dark and simulated sunlight conditions, were used to determine the corresponding uptake coefficients (γ_{ss}) and product yields.

1.4.2. *Uptake coefficients and data analysis*

The uptake coefficient of NO_2 on the v-dust surface can be derived from the following expression:

$$\gamma_{geom} = \frac{2 \times k_{kin} \times r_{tube}}{C_{NO2}} \quad (1)$$

where γ_{geom} is the geometric uptake coefficient, k_{kin} (sec^{-1}) is the first order reaction rate loss of gas-phase NO_2 in the kinetic regime, r_{tube} is the radius of the tube, and C_{NO2} (cm/sec) is the average molecular velocity. Both the radius of the tube (0.49 cm) and the average molecular speed at 293 K are known parameters, therefore only k_{kin} needs to be determined. Further information about the calculations of uptake coefficients and diffusion corrections can be retrieved elsewhere (Romanias et al., 2013, 2012; Tang et al., 2014) and are also given in Appendix A. Supplementary data.

The determination of the uptake coefficient using the geometric surface area (S_{geom}) can be considered as an upper limit (Crowley et al., 2010). An alternative way for the calculation of the uptake coefficient is using the specific surface area (A_s) of the solid, considering that all surface sites are accessible to the gas phase molecules. For the determination of the specific surface area (SSA), the Brunauer-Emmett-Teller (BET) isotherm approach is applied and the corresponding uptake coefficient (γ_{BET}) is given by the following expression:

$$\gamma_{BET} = \frac{\gamma_{geom} \times S_{geom}}{S_{BET}} \quad (2)$$

where S_{BET} (m^2/g) is the product of the specific surface area (A_s) of the solid with the deposited mass (g).

2. Results and discussion

2.1. *Determination of NO_2 uptake coefficients on v-dust samples*

This section includes the results of the kinetic measurements performed under simulated atmospheric conditions aiming to determine the uptake coefficients of NO_2 on the volcanic samples. Initially, the impact of experimental conditions on the uptake is discussed using dust from Hagavatn collection spot as a model volcanic sample; this choice is based on two criteria. First, Hagavatn dust hot spot is in close vicinity to Reykjavik - the most densely populated area in Iceland - and secondly, the air quality in Reykjavik is very frequently impacted from massive loads of v-dust particles originating from Hagavatn dust hot spot. Therefore, it was considered as the most representative sample to study with the ultimate objective to evaluate the corresponding impacts of NO_2 aged volcanic dust to the chemistry of the local/regional atmosphere. Finally, at the end of this section a thorough comparison between the uptake coefficients determined on the five volcanic samples under the same experimental conditions is performed.

2.1.1. *Dependence of NO_2 uptake coefficient on the sample mass*

In this series of experiments, the steady state uptake coefficient was investigated as a function of Hagavatn v-dust mass exposed to the NO_2 flow. The objective was to determine the v-dust surface area involved in the interaction with NO_2 molecules. The experiments were performed under both dark and simulated sunlight irradiation conditions ($J_{NO2} = 4.5 \times 10^{-3}$ sec^{-1}) at temperature (T) = 293 K, 100 ppbV of NO_2 and dry conditions. The obtained results are presented in Appendix A Fig. S3. A linear increase of the geometric uptake coefficient ($\gamma_{ss,geom}$) was observed as a function of the mass of Hagavatn coated on the tube. This trend points out that the entire surface area of the solid sample is accessible to NO_2, and consequently, the BET specific surface area should be used for the determination of the true uptake coefficient (Crowley et al., 2010). Furthermore, under UV light conditions, the observed linear increase also indicates that the sample surface is homogeneously irradiated, irrespectively of the sample mass

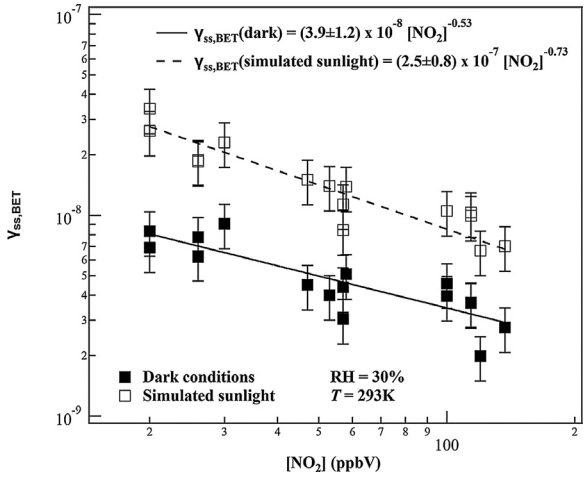

Fig. 4 – Uptake coefficients of NO_2 ($\gamma_{ss,BET}$) on Hagavatn volcanic sample as a function of initial concentration under dark ($\gamma_{ss,BET}$ (dark)) and simulated sunlight irradiation ($\gamma_{ss,BET}$ (simulated sunlight)). Error bars denote the overall uncertainty on $\gamma_{ss,BET}$ determination (ca. 25%) that arise mostly from the determination of specific surface area (SSA). Temperature was set at T = 293 K, and relative humidity (RH) = 30%.

(Herrmann, 2005). Similar trends were observed for the remaining volcanic samples and have been also reported in literature for mineral oxides and natural mineral dusts (El Zein et al., 2013a, 2013b; Romanias et al., 2016; Zein et al., 2014).

2.1.2. *Dependence of uptake coefficients on the irradiance intensity*

To evidence potential photocatalytic or photoinduced processes on the surface of the volcanic samples, the irradiance intensity of the incident light was varied inside the reactor. The experiments were carried out at 30% of RH, 293 K using 20 ppbV of NO_2 as inlet concentration and the steady-state uptake coefficient was measured as a function of the number of UV lamps switched on, varying from 0 to 3 lamps. Appendix A Fig. S4 displays the results on Hagavatn sample. A linear increase of the uptake coefficient with the irradiance intensity was observed. It varied almost by a factor of 10 comparing the values under dark and 3 UV lamps, pointing out that NO_2 degradation rate is linearly driven by the radian flux (Herrmann, 2005). However, if photons clearly induce specific photoactivated phenomena on the v-dust surfaces it cannot be determined at this point whether they are photocatalytic or photochemical. Nevertheless, similar trends have been noted in literature for mineral oxides and natural mineral dusts (El Zein and Bedjanian, 2012; Tang et al., 2017; Zein et al., 2014).

2.1.3. *Dependence of uptake coefficients on NO_2 concentration*

The dependence of the steady state uptake coefficient on the inlet concentration of NO_2 was studied in the range of 20–140 ppbV. In this set of experiments Hagavatn volcanic sample was exposed to NO_2 at T = 293 K, 30% of RH under both dark and UV irradiation conditions and the results are displayed in Fig. 4. The simulated sunlight irradiation of the surface has promoted the uptake of NO_2 by a factor of three in the entire concentration range. Furthermore, under both dark and light conditions, the uptake coefficient was found to be almost constant for concentrations below 40 ppbV, however, above that limit a slight decrease was observed; the latter may be attributed to the surface saturation by the adsorbed inter-

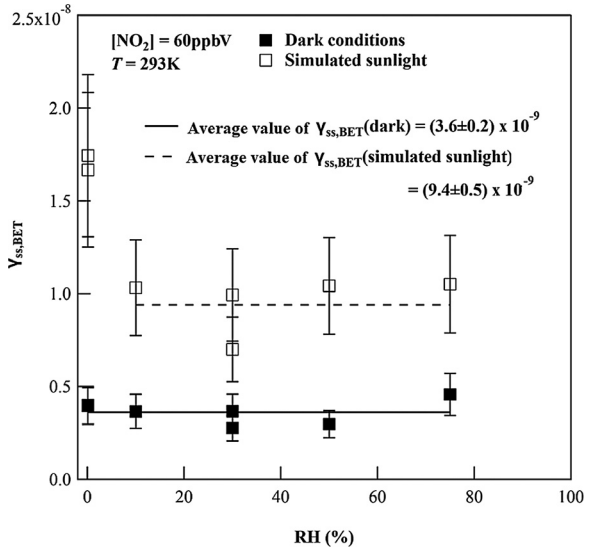

Fig. 5 – Uptake coefficients of NO_2 on Hagavatn volcanic sample as a function of relative humidity under darkand simulated sunlight irradiation. Error bars reflects the overall uncertainty on $\gamma_{ss,BET}$ determination (ca. 25%) that arise mostly from the determination of SSA.

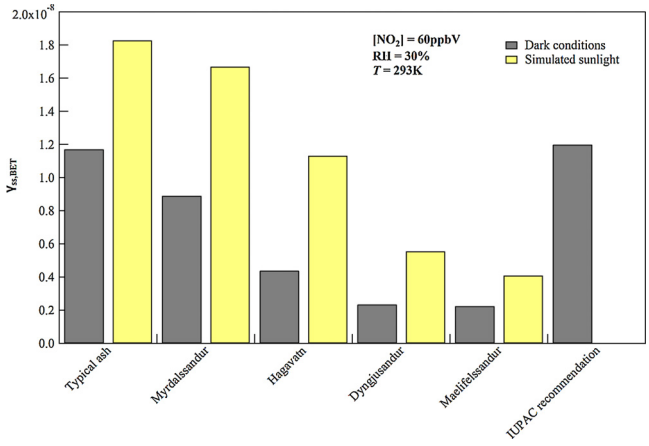

Fig. 6 – Uptake coefficients of NO_2 as a function of volcanic samples origin under dark and simulated sunlight irradiation. For comparison purposes, the recommended uptake coefficient value proposed by the International Union of Pure and Applied Chemistry (IUPAC) panel for mineral oxides under dark and dry conditions is given.

mediates. The solid lines of Fig. 4 correspond to the empirical power fit of results according to the following expressions:

$$\gamma_{ss,BET}(\text{dark}) = (3.9 \pm 1.2) \times 10^{-8}[NO_2]^{-0.53} \quad (3)$$

$$\gamma_{ss,BET}(\text{simulated sunlight}) = (2.5 \pm 0.8) \times 10^{-7}[NO_2]^{-0.73} \quad (4)$$

where $\gamma_{ss,\ BET}$(dark) and $\gamma_{ss,\ BET}$(simulated sunlight) refer to dark and simulated sunlight conditions, respectively, and $[NO_2]$ (ppbV) is the initial concentration of NO_2. The quoted uncertainties correspond to the two sigma (2σ) precision of the fit of experimental results. Therefore, one can extrapolate the uptake coefficient of NO_2 at any tropospheric concentration range.

2.1.4. *Dependence of NO_2 uptake coefficient on RH*

The uptake coefficients of NO_2 on Hagavatn sample were determined as a function of relative humidity from dry conditions to 75% RH, the results are displayed in Fig. 5. Aiming to isolate the effect of RH on the kinetic parameter, in this series of experiments the volcanic sample was always exposed to 60 ppbV of NO_2 at 293 K. Under dark conditions, the steady state uptake coefficient was found to be independent of RH in the whole investigated RH range. The solid black line in Fig. 5, corresponds to the mean value of the steady state coefficient in the entire RH range:

$$\gamma_{ss,BET}(\text{dark}) = (3.6 \pm 0.2) \times 10^{-9} \quad (5)$$

The quoted uncertainties correspond to the 2σ precision of the fit of experimental results.

As shown in Fig. 5, the UV irradiation of the sample surface promoted the consumption of NO_2 in the entire RH range compared to dark conditions; the $\gamma_{ss,BET}$ under simulated sunlight was promoted by a factor of 3 compared to dark and was found to be independent of RH under ambient relative humidity conditions i.e., RH higher than 10%. The dash black line in Fig. 5, corresponds to the mean value of the steady state coefficient for ambient RH conditions:

$$\gamma_{ss,BET}(\text{simulated sunlight}) = (9.4 \pm 0.5) \times 10^{-9} \quad (6)$$

Interestingly, under dry conditions, the enhancement of $\gamma_{ss,BET}$ upon surface irradiation was by a factor of 6.

The independent nature of $\gamma_{ss,BET}$ on RH does not preclude that water molecules do not affect the reaction mechanism. More precisely, under UV light irradiation, H_2O is a well-known source of radicals (i.e., $\cdot OH$, $O_2^{-\cdot}$) on mineral dust surfaces that contain photocatalysts (Chen et al., 2012; Herrmann, 2005; Romanias et al., 2012; Schneider et al., 2014), and thus, enhance the reactivity of the surface towards NO_2 (Herrmann, 2005; Romanias et al., 2012; Zein et al., 2014). On the other hand, adsorbed water may also block some sorptive and reactive sites and induce a decrease to $\gamma_{ss,BET}$ (Romanias et al., 2012, 2017; Zein et al., 2014). It seems that under ambient RH conditions (RH > 30%), the effect of sites blocking by water is probably compensated by its role as a source of radical species on the surface of the dust. Under dark conditions, radical species are not expected to be formed. However, the disproportionation of NO_2 can occur on the surface of the volcanic sample leading to a continuous consumption of NO_2 (Finlayson-Pitts et al., 2003). Further details regarding the reaction mechanism under both dark and light conditions versus relative humidity are given in reaction mechanism section.

2.1.5. *Comparison of NO_2 uptake coefficients on various volcanic samples under defined experimental conditions*

Aiming to compare the uptake coefficients of NO_2 on the different volcanic samples a series of experiments were carried out under defined and atmospheric experimental conditions: 30% RH, NO_2 concentration 60 ppbV, under both dark and simulated sunlight. The results obtained are displayed in Fig. 6, where for comparison purposes the international union of pure and applied chemistry, International Union of Pure and Applied Chemistry (IUPAC) recommended value on mineral oxides is also displayed. A significant variation of the $\gamma_{ss,BET}$ as a function of the origin of the samples can be noted. In addition, the simulated sunlight radiation of the volcanic samples induced an increase to the $\gamma_{ss,BET}$ for all samples indicating the existence of photo-induced processes on the surface of all dusts.

The dependence noted on the $\gamma_{ss,BET}$ values from one volcanic sample to another is significant. Despite the fact that samples originate from close geographical regions, the

chemical composition of the magma that produced them is different (see Appendix A. Supplementary data), and thus, variations in the composition of the natural samples and contrasted surface properties are expected. Furthermore, taking into account that their crystalline fraction is relatively low, ca. 20% for all samples beside Hagavatn, it makes any correlation between mineralogical composition and reactivity challenging. The relative abundance of elements could have been a base for comparison, however, it is quite similar for all samples, and no relevant correlation trends were noticed.

Interestingly, a correlation between the uptake coefficients and the specific surface area was noticed for both dark and light conditions (Appendix A Fig. S5); the highest the specific surface area, the lowest the uptake coefficient. The latter could indicate that morphological parameters can play an important role and affect the surface properties of the samples studied. It has been shown that the specific surface area is inversely correlated with the particles size in literature (Ibrahim et al., 2018) – and that small particles are more irregular. Moreover, it has been evidenced that the water monolayer is formed at lower RH for natural mineral samples with small particle sizes due to higher OH group surface density (Ibrahim et al., 2018; Tang et al., 2016). Therefore, a possible explanation could be that the NO_2 uptake or/and the abundance of intermediate surface species formed are influenced by the presence of surface OH group density.

The $\gamma_{ss,BET}$ values measured for the volcanic samples are in the same order of magnitude but relatively lower than the IUPAC recommendation. However, it should be stressed out that the IUPAC recommended value is based on studies performed with mineral oxides and not natural samples under low pressure and dry conditions, although RH is a governing factor for NO_2 uptake. Recent studies performed on oxides and natural or synthetic mineral dusts report uptake coefficients of NO_2 in the order of 10^{-9} (Crowley et al., 2010; Li et al., 2010; Ndour et al., 2009), and thus, similar or even lower than those determine in the current study.

2.2. *Investigation of products formed along with NO_2 uptake*

The results presented in this section concern the determination of the gas-phase products of NO_2 interaction with the volcanic surfaces. The yield of the detected products (PY) was determined as the ratio of the product concentration formed (Δ[product]) to the concentration of NO_2 consumed ($\Delta[NO_2]$) after achieving steady state conditions:

$$PY = \Delta[\text{product}]/\Delta[NO_2] \quad (7)$$

To investigate the impact of experimental conditions, Hagavatn volcanic sample was used as model volcanic sample. Finally, at the end of the section the product yields determined for all volcanic samples under defined experimental conditions are presented and discussed.

2.2.1. *Product yield as a function of NO_2 initial concentration and relative humidity*

The impact of experimental conditions, such as NO_2 initial concentration (in the range of 40–140 ppbV) and relative humidity (from dry to 75% RH) on the yield of the products formed was investigated at room temperature, under both dark and simulated sunlight, using Hagavatn as model surface sample. In all cases, NO and HONO were measured as the only nitrogen containing gas phase products. Regarding concentration dependence, the experiments were carried out at 30% of RH and the yields of NO and HONO were 40% ± 10% and 60% ± 10%, respectively, independent on NO_2 initial concentration. The product yield measurements as a function of RH were carried out at 60 ppbV of initial NO_2. As displayed in Fig. 7, NO and HONO were detected as primary gas phase products, with almost identical values under both dark and simulated sunlight conditions, however, their formation was highly dependent on relative humidity. As relative humidity increases, the formation of HONO is favored while that of NO is diminished. The latter is in accordance with the literature where similar trends have been reported for mineral oxides (Baltrusaitis et al., 2009; Bedjanian and El Zein, 2012) and results seems to justify the mechanism proposed about enhanced formation of HONO on humid surfaces (Finlayson-Pitts et al., 2003; Rodriguez et al., 2001). In addition, for RH above 20% a nitrogen mass balance evidenced the complete conversion of adsorbed NO_2 to the gas phase products. However, for RH below 10%, the nitrogen mass balance was not completed only considering the gas phase products, thus, the presence of nitrogen containing species on the surface, i.e., adsorbed NO_2 or surface reaction products, is expected. The latter indicates that water plays a key role on the sorption and/or reaction mechanism facilitating the transformation of NO_2 to gas phase products. Similar formation yields and trend were noticed for the other volcanic samples and have been also reported in literature on the surface of mineral oxides and natural desert dusts (Bedjanian and El Zein, 2012; Tang et al., 2017).

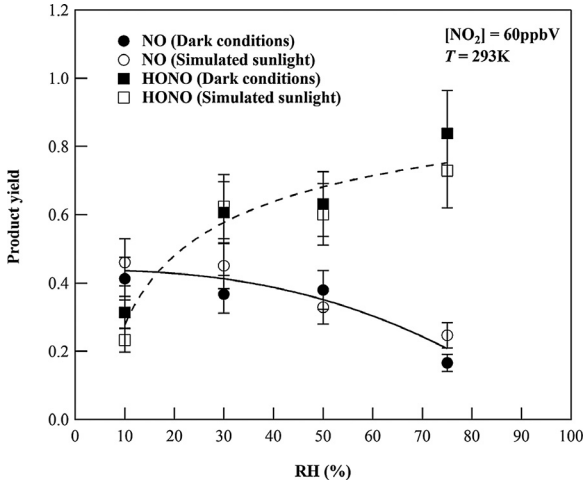

Fig. 7 – Product yields of NO (cycles) and HONO (squares) formation determined as a function of relative humidity upon reaction of NO_2 with Hagavatn volcanic sample under dark and simulated sunlight radiation. Error bars reflects the overall uncertainty on the product yields (ca. 15%). The solid and dashed lines are the empirical fit of experimental results (both dark and simulated sunlight) to demonstrate the corresponding trends of NO and HONO yields versus RH.

2.2.2. *NO and HONO product yields on various volcanic samples under defined experimental conditions*

In this series of experiments the volcanic samples were exposed to 60 ppbV concentration of NO_2, 30% of RH under both dark and simulated sunlight irradiation conditions. The results are presented in Table 1. Considering the experimental uncertainties, no significant variation was noticed to the formation yield of NO between the 5 volcanic samples under dark and simulated sunlight conditions although significant differences were observed for the uptake coefficients. On the contrary, the HONO formation yields for Eyjafjallajökull

Table 1 – Product yields of NO and HONO determined for the five volcanic samples under fixed experimental conditions [NO_2] = 60 ppbV and RH = 30% under dark and simulated sunlight radiation.

Volcanic sample	Yield NO		Yield HONO		Total yield	
	Dark	Light	Dark	Light	Dark	Light
Eyjafjallajökull typical ash	28% ± 4%	48% ± 7%	71% ± 11%	53% ± 8%	99% ± 15%	101% ± 15%
Mýrdalssandur	22% ± 3%	44% ± 7%	52% ± 8%	56% ± 8%	74% ± 11%	100% ± 15%
Hagavatn	37% ± 6%	45% ± 7%	60% ± 9%	62% ± 9%	97% ± 15%	107% ± 16%
Dyngjusandur	39% ± 6%	50% ± 8%	37% ± 6%	38% ± 6%	76% ± 11%	88% ± 13%
Maelifellssandur	28% ± 4%	37% ± 6%	48% ± 7%	47% ± 7%	76% ± 11%	84% ± 13%

typical ash, Mýrdalssandur and Hagavatn, were systematically higher than those measured for Dyngjusandur and Maelifellssandur v-dusts. Interestingly, it seems that HONO formation in the gas phase is promoted on volcanic dusts with higher NO_2 uptake coefficients.

In addition, the irradiation of the surface increased the formation of NO for all samples while the HONO yield was not influenced. The latter observation suggests that (i) either surface adsorbed nitrogen species are photolysed or (ii) the surface is photoactivated and photocatalytic processes occur, leading to the formation of NO. It should be noted that HONO photolysis in the gas phase is not expected to occur in our system since the photolysis frequency of HONO is almost one order of magnitude slower than NO_2, thus, it is not expected to occur in our reactor, and HONO yields didn't decrease upon surface irradiation. Concerning the total formation yields of gas phase products, under surface irradiation a systematic increase was observed (except for typical ash sample) compared with dark conditions, leading to an almost completion of the nitrogen mass balance for all samples within the experimental uncertainties.

2.3. *Proposed reaction mechanism*

2.3.1. *Dark conditions*

The heterogeneous degradation of NO_2 on the surface of volcanic samples resulted in the formation of both NO and HONO in the gas phase. Several pathways have been proposed to occur for the transformation of NO_2 on mineral surfaces. In particular, NO_2 can be initially physisorbed on metal sites (SS^n stands for surface site) of the mineral surface (Eq. (8)) and then disproportionate (Eq. (9)), leading to the formation of surface nitrates (Eq. (9)) and gaseous NO (Eq. (10)) (Finlayson-Pitts et al., 2003; Rodriguez et al., 2001). Furthermore, NO_2 can directly react with surface O atoms, SS-O, and form surface nitrates (Eq. (11)) (Baltrusaitis et al., 2009). Alternatively NO_2 can be chemisorbed and reduced to NO_2^- by metal sites, i.e., ferrous iron sites Fe^{2+}, expected to be relatively abundant in the volcanic samples, in an electron transfer reaction that is facilitated by adsorbed water (Eqs. (12) and (13)) leading to HONO formation (Kebede et al., 2016). In the presence of water, the abundance of surface OH groups increases, SS-OH (Ibrahim et al., 2018; Joshi et al., 2017; Tang et al., 2016), and according to literature, NO_2 can form a hydrogen bond stabilized ONOOH species that could either lead to the formation of gas HONO or isomerize and form adsorbed nitric acid (Eqs. (14) and (15)) (Baltrusaitis et al., 2009).

$$SS^n + NO_{2(g)} \leftrightarrow SS^n\text{-}NO_{2(ads)} \quad (8)$$

$$2\,[SS^n\text{-}NO_{2(ads)}] \rightarrow SS^n\text{-}NO_3^-{}_{(ads)} + SS^n\text{-}NO^+{}_{(ads)} \quad (9)$$

$$SS^n\text{-}NO^+{}_{(ads)} \rightarrow SS^n + NO_{(g)} \quad (10)$$

$$SS\text{-}O + NO_{2(g)} \rightarrow SS^{n+1}\text{-}NO_3^-{}_{(ads)} \quad (11)$$

$$SS^n + NO_{2(g)} \rightarrow SS^{n+1}\text{-}NO_2^-{}_{(ads)} \quad (12)$$

$$SS^{n+1}\text{-}NO_2^-{}_{(ads)} + H^+ \rightarrow SS^n\text{-}HONO_{(ads)} \quad (13)$$

$$SS\text{-}OH + NO_{2(g)} \rightarrow SS\text{-}ONOOH_{(ads)} \rightarrow SS\text{-}O + HONO_{(gas)} \quad (14)$$

$$SS - ONOOH \xrightarrow{\text{Isomerization}} SS - HNO_3 \quad (15)$$

The proposed reaction mechanism is in agreement with our experimental observations. Under dry conditions, the dominant reaction pathways are: the disproportionation of NO_2, leading to high formation yields of $NO_{(g)}$ (Eqs. (8)–(10)); and reactions (11) and (12), respectively, forming surface nitrates and nitrites. Reactions (13)–(15) are still active pathways even under dry conditions, since the removal of strongly adsorbed surface water requires a stronger thermal pretreatment method (> 500 K) than the one followed in our study (Joshi et al., 2017). Consequently, the sequence of reactions proposed seems to explain the high formation yields of NO, and the corresponding low HONO yields observed for Hagavatn sample under dry conditions, as well as the absence of nitrogen mass balance of the gas products due to the formation of surface adsorbed nitrogen containing species.

By increasing the relative humidity, the surface density of OH groups also increases considerably (especially after water monolayer formation that is expected at RH greater than 25%–30% RH, (Joshi et al., 2017), and thus, reactions (13)–(15) which are competing to reactions (8), (9), (11) and (12), become the dominant pathways leading to an enhanced formation of HONO. Consequently, the formation of NO is diminished similar with the concentration of surface adsorbed species and a nitrogen mass balance is observed.

2.3.2. *UV light conditions*

Under simulated sunlight irradiation of the surface, and comparing the results obtained under fixed experimental conditions (i.e., fixed NO_2 concentration and 30% RH - see Table 1) the uptake of NO_2 was enhanced, however unlike HONO the yield of NO was significantly influenced. These observations could possibly point to the presence of photo-induced processes on the surface of volcanic samples. Note that photocatalytic processes could also take place but considering that the detailed mineralogical composition of the volcanic samples is not known and that samples are mostly amorphous, the consideration of these processes is speculative and that they are not considered in the proposed reaction mechanism.

The surface adsorbed nitrite species formed under dark conditions through reaction (12) could be photolysed in presence of simulated sunlight ($h\nu$) producing gaseous NO and regenerating a SS-O surface site according to reaction:

$$SS^{n+1}\text{-}NO_2^-{}_{(ads)} + h\nu \rightarrow SS\text{-}O + NO_{(g)} \quad (16)$$

Similarly, nitrates formed through reaction (11) can be the source of gaseous NO and NO_2 through reactions (17) and (18):

$$SS^{n+1}\text{-}NO_3^-{}_{(ads)} + h\nu \rightarrow SS^n + NO_{(g)} + O_2 \quad (17)$$

$$SS^{n+1}\text{-}NO_3^-{}_{(ads)} + h\nu \rightarrow SS\text{-}O + NO_{2(g)} \quad (18)$$

Reaction pathways (16)–(18) corroborate the photoinduced consumption of NO_2 under simulated sunlight conditions, as well as the slight but systematic photoenhanced formation of NO observed on volcanic samples under 30% of RH.

3. Conclusions and atmospheric implications

Within the framework of the current study, the reactivity of Icelandic volcanic samples towards NO_2 was studied as a function of several atmospheric parameters. Despite the relative close regions where the samples were collected, the uptake coefficients varied significantly from one sample to another. It is suggested that the origin of the magma and morphological differences between the samples could possibly explain the variations noted. Besides the kinetics, the formation yields of NO and HONO were also determined. The relative humidity was found to influence the balance between adsorbed and gas phase products as well as the distribution of NO and HONO yields. Interestingly, under atmospheric conditions (i.e., > 30% RH, ambient temperature) higher HONO formation yields were noticed for the volcanic samples. Finally, based on the experimental observations of the current study, a reaction mechanism was proposed.

Regarding the atmospheric implications, we estimate that the corresponding impacts of NO_2 transformation to HONO is expected to be significant in cases of volcanic eruptions or during more frequent events such as volcanic dust storms. Indeed, using Iceland as a case study, it has been evidenced that volcanic dust storms are much more frequent than volcanic eruptions transporting volcanic aerosols to central Europe or Arctic (Dagsson-Waldhauserova et al., 2014a). Interestingly, about half of these events occur in winter (dark season) when NO_2 concentrations in Reykjavik can exceed 60 ppbV.

In an attempt to estimate the atmospheric significance of NO_2 heterogeneous degradation on volcanic particles, the rate coefficient of NO_2 heterogeneous loss (k_{het} (hr^{-1})) was calculated from the following equation:

$$k_{het} = \frac{\gamma \times c \times A}{4} \quad (19)$$

where, γ is the NO_2 uptake coefficient, c (cm/hr) is the mean molecular velocity, and A (cm^2/cm^3) is the aerosol surface area density. Using Iceland as case study, under typical PM_{10} concentrations during a v-dust storm, i.e., ca. 300 µg/m^3 (Arnalds et al., 2016, 2014; Dagsson-Waldhauserova et al., 2015; Thorsteinsson et al., 2011), RH greater than 70%, NO_2 concentrations of ca 8 ppbV (annual average values) (Hazenkamp-von Arx et al., 2004) and extrapolating the uptake coefficient of NO_2 under dark conditions corresponding to winter season using Eq. (3), the heterogeneous loss of NO_2 is relatively low (in the order of 10^{-6} hr^{-1}) and the estimated HONO formation rate is not expected to exceed 0.1 pptV/hr. Even considering the peak NO_2 concentration of 60 ppbV the HONO formation rate is below 0.3 pptV/hr. However, during severe dust events (7000 µg/m^3), the heterogeneous loss of NO_2 could be substantially higher (up to 10^{-4} hr^{-1}) and HONO formation rate could reach 4 pptV/hr. Considering the severe dust event scenario during the summer season up to 10 pptV/hr of HONO can be expected, and thus, a significant impact to the oxidative capacity of the regional atmosphere.

To conclude, the significance of NO_2 scavenging on the surface of volcanic particles is mainly dependent on the v-dust atmospheric loads. Nevertheless, this study clearly evidences that volcanic dust particles can efficiently uptake, scavenge and transform NO_2. Similar trends could be expected for other pollutants. Indeed, in the recent study of Urupina et al. (2019) it was evidenced an efficient uptake and transformation of sulfur dioxide to sulfates on these Icelandic volcanic dusts. Therefore, Icelandic v-dust aerosols should be considered as reactive components of the atmosphere; In the context of their long range transportation to Europe and especially Arctic it is expected to transport, scavenge and transform pollutants, and thus, to alter the corresponding air quality and chemistry of the atmosphere.

Declaration of competing interest

The authors declare that they have no known competing financial interests or personal relationships that could have appeared to influence the work reported in this paper.

Acknowledgments

This work was achieved in the frame of Labex chemical and physical properties of the atmosphere (Labex CaPPA) project, funded by agence nationale de la recherché (ANR) through the program d'investissements d'avenir (PIA) (No. ANR-11-LABX-0005-01), and contrat de plan état-région changement climatique dynamique de l'atmosphère impacts sur la biodiversité et la santé humaine (CPER CLIMIBIO) project, funded by the hauts-de-france regional council and the european regional development fund (ERDF). Work of Pavla Dagsson-Waldhauserova was partly funded by the Czech Science Foundation under the 'the role of high latitude dust in changing climate' (HLD-CHANGE) project (No. 20-06168Y). Manolis N. Romanias is thankful to the INSU LEFE-CHAT program for financial support.

Appendix A. Supplementary data

Supplementary material associated with this article can be found in the online version at doi:10.1016/j.jes.2020.03.042.

REFERENCES

Arnalds, O., Dagsson-Waldhauserova, P., Olafsson, H., 2016. The Icelandic volcanic aeolian environment: processes and impacts - a review. Aeolian Res. 20, 176–195.
Arnalds, O., Olafsson, H., Dagsson-Waldhauserova, P., 2014. Quantification of iron-rich volcanogenic dust emissions and deposition over the ocean from Icelandic dust sources. Biogeosciences 11, 6623–6632.
Arnalds, O., Thorarinsdottir, E.F., Thorsson, J., Waldhauserova, P.D., Agustsdottir, A.M., 2013. An extreme wind erosion event of the fresh Eyjafjallajökull 2010 volcanic ash. Sci. Rep. 3, 1257.
Auker, M.R., Sparks, R.S.J., Siebert, L., Crosweller, H.S., Ewert, J., 2013. A statistical analysis of the global historical volcanic fatalities record. J. Appl. Volcanol. 2, 2.
Baltrusaitis, J., Jayaweera, P.M., Grassian, V.H., 2009. XPS study of nitrogen dioxide adsorption on metal oxide particle surfaces under different environmental conditions. Phys. Chem. Chem. Phys. 11, 8295–8305.
Baratoux, D., Mangold, N., Arnalds, O., Bardintzeff, J-M., Platevoët, B., Grégoire, M., et al., 2011. Volcanic sands of Iceland - Diverse origins of aeolian sand deposits revealed at Dyngjusandur and Lambahraun. Earth Surf. Process. 36, 1789–1808.
Barnard, J.C., Chapman, E.G., Fast, J.D., Schmelzer, J.R., Slusser, J.R., Shetter, R.E., 2004. An evaluation of the FAST-J photolysis algorithm for predicting nitrogen dioxide photolysis rates under clear and cloudy sky conditions. Atmos. Environ. 38, 3393–3403.
Bedjanian, Y., El Zein, A., 2012. Interaction of NO_2 with TiO_2 surface under UV irradiation: products study. J. Phys. Chem. A 116, 1758–1764.
Bohn, B., Rohrer, F., Brauers, T., Wahner, A., 2005. Actinometric measurements of NO_2 photolysis frequencies in the atmosphere simulation chamber SAPHIR. Atmos. Chem. Phys. 5, 493–503.

Boichu, M., Chiapello, I., Brogniez, C., Pere, J.C., Thieuleux, F., Torres, B., et al., 2016. . Current challenges in modelling far-range air pollution induced by the 2014-2015 Baroarbunga fissure eruption (Iceland). Atmos. Chem. Phys. 16, 10831–10845.
Butwin, M.K., von Löwis, S., Pfeffer, M.A., Thorsteinsson, T., 2019. The effects of volcanic eruptions on the frequency of particulate matter suspension events in Iceland. J. Aerosol Sci. 128, 99–113.
Chen, H., Nanayakkara, C.E., Grassian, V.H., 2012. Titanium dioxide photocatalysis in atmospheric chemistry. Chem. Rev. 112, 5919–5948.
Crowley, J.N., Ammann, M., Cox, R.A., Hynes, R.G., Jenkin, M.E., Mellouki, A., et al., 2010. Evaluated kinetic and photochemical data for atmospheric chemistry: Volume V – heterogeneous reactions on solid substrates. Atmos. Chem. Phys. 10, 9059–9223.
Dagsson-Waldhauserova, P., Arnalds, O., Olafsson, H., 2014a. Long-term variability of dust events in Iceland (1949–2011). Atmos. Chem. Phys. 14, 13411–13422.
Dagsson-Waldhauserova, P., Arnalds, O., Olafsson, H., Skrabalova, L., Sigurdardottir, G.M., Branis, M., et al., 2014b. Physical properties of suspended dust during moist and low wind conditions in Iceland. Icel. Agric. Sci. 27, 25–39.
Dagsson-Waldhauserova, P., Arnalds, O., Olafsson, H., Hladil, J., Skala, R., Navratil, T., et al., 2015. Snow–dust storm: unique case study from Iceland, March 6–7, 2013. Aeolian Res. 16, 69–74.
Dagsson-Waldhauserova, P., Magnusdottir, A.O., Olafsson, H., Arnalds, O., 2016. The spatial variation of dust particulate matter concentrations during two icelandic dust storms in 2015. Atmos. Basel 7 (6), 77.
Đorđević, D., Tošić, I., Sakan, S., Petrović, S., Đuričić-Milanković, J., Finger, D.C., et al., 2019. Can volcanic dust suspended from surface soil and deserts of Iceland be transferred to Central Balkan similarly to African dust (Sahara)? Front. Earth Sci. 7, 142.
El Zein, A., Bedjanian, Y., 2012. Interaction of NO_2 with TiO_2 surface under UV irradiation: measurements of the uptake coefficient. Atmos. Chem. Phys. 12, 1013–1020.
El Zein, A., Bedjanian, Y., Romanias, M.N., 2013a. Kinetics and products of HONO interaction with TiO_2 surface under UV irradiation. Atmos. Environ. 67, 203–210.
El Zein, A., Romanias, M.N., Bedjanian, Y., 2013b. Kinetics and products of heterogeneous reaction of HONO with Fe_2O_3 and Arizona test dust. Environ. Sci. Technol. 47, 6325–6331.
Engelstaedter, S., Tegen, I., Washington, R., 2006. North African dust emissions and transport. Earth Science Rev. 79, 73–100.
Finlayson-Pitts, B.J., Wingen, L.M., Sumner, A.L., Syomin, D., Ramazan, K.A., 2003. The heterogeneous hydrolysis of NO_2 in laboratory systems and in outdoor and indoor atmospheres: an integrated mechanism. Phys. Chem. Chem. Phys. 5, 223–242.
George, C., Ammann, M., D'Anna, B., Donaldson, D.J., Nizkorodov, S.A., 2015. Heterogeneous photochemistry in the atmosphere. Chem. Rev. 115, 4218–4258.
Gislason, S.R., Hassenkam, T., Nedel, S., Bovet, N., Eiriksdottir, E.S., Alfredsson, H.A., et al., 2011. Characterization of Eyjafjallajökull volcanic ash particles and a protocol for rapid risk assessment. Proc. Nat. Acad. Sci. 108, 7307.
Groot Zwaaftink, C.D., Arnalds, Ó., Dagsson-Waldhauserova, P., Eckhardt, S., Prospero, J.M., Stohl, A., 2017. Temporal and spatial variability of Icelandic dust emissions and atmospheric transport. Atmos. Chem. Phys. 17, 10865–10878.
Gudmundsson, M.T., Thordarson, T., Höskuldsson, Á., Larsen, G., Björnsson, H., Prata, F.J., et al., 2012. Ash generation and distribution from the April-May 2010 eruption of Eyjafjallajökull, Iceland. Sci. Rep. 2, 572.
Hazenkamp-von Arx, M.E., Götschi, T., Ackermann-Liebrich, U., Bono, R., Burney, P., Cyrys, J., et al., 2004. $PM_{2.5}$ and NO_2 assessment in 21 European study centres of ECRHS II: annual means and seasonal differences. Atmos. Environ. 38, 1943–1953.
Herrmann, J.M., 2005. Heterogeneous photocatalysis: state of the art and present applications. Top. Catal. 34, 49–65.
Ibrahim, S., Romanias, M.N., Alleman, L.Y., Zeineddine, M.N., Angeli, G.K., Trikalitis, P.N., et al., 2018. Water interaction with mineral dust aerosol: particle size and hygroscopic properties of dust. ACS Earth Space Chem. 2, 376–386.
Ilyinskaya, E., Schmidt, A., Mather, T.A., Pope, F.D., Witham, C., Baxter, P., et al., 2017. Understanding the environmental impacts of large fissure eruptions: aerosol and gas emissions from the 2014–2015 Holuhraun eruption (Iceland). Earth Planet. Sci. Lett. 472, 309–322.
Joshi, N., Romanias, M.N., Riffault, V., Thevenet, F., 2017. Investigating water adsorption onto natural mineral dust particles:linking DRIFTS experiments and BET theory. Aeolian Res. 27, 35–45.
Kebede, M.A., Bish, D.L., Losovyj, Y., Engelhard, M.H., Raff, J.D., 2016. The role of iron-bearing minerals in NO_2 to HONO conversion on soil surfaces. Environ. Sci. Technol. 50, 8649–8660.
Kleffmann, J., 2007. Daytime sources of nitrous acid (HONO) in the atmospheric boundary layer. ChemPhysChem 8, 1137–1144.
Lasne, J., Romanias, M.N., Thevenet, F., 2018. Ozone uptake by clay dusts under environmental conditions. ACS Earth Space Chem. 2, 904–914.
Li, H.J., Zhu, T., Zhao, D.F., Zhang, Z.F, Chen, Z.M., 2010. Kinetics and mechanisms of heterogeneous reaction of NO_2 on $CaCO_3$ surfaces under dry and wet conditions. Atmos. Chem. Phys. 10, 463–474.
Mellouki, A., Wallington, T.J., Chen, J., 2015. Atmospheric chemistry of oxygenated volatile organic compounds: impacts on air quality and climate. Chem. Rev. 115, 3984–4014.
Moroni, B., Arnalds, O., Dagsson-Waldhauserová, P., Crocchianti, S., Vivani, R., Cappelletti, D., 2018. Mineralogical and chemical records of Icelandic dust sources upon Ny-Ålesund (Svalbard Islands). Front. Earth Sci. 6 (187), 1–13.
Nault, B.A., Garland, C., Wooldridge, P.J., Brune, W.H., Campuzano-Jost, P., Crounse, J.D., et al., 2016. Observational constraints on the oxidation of NOx in the upper troposphere. J. Phys. Chem. A 120, 1468–1478.
Ndour, M., Nicolas, M., D'Anna, B., Ka, O., George, C., 2009. Photoreactivity of NO_2 on mineral dusts originating from different locations of the Sahara desert. Phys. Chem. Chem. Phys. 11, 1312–1319.
Ovadnevaite, J., Ceburnis, D., Plauskaite-Sukiene, K., Modini, R., Dupuy, R., Rimselyte, I., et al., 2009. Volcanic sulphate and arctic dust plumes over the North Atlantic Ocean. Atmos. Environ. 43, 4968–4974.
Perring, A.E., Pusede, S.E., Cohen, R.C., 2013. An observational perspective on the atmospheric impacts of alkyl and multifunctional nitrates on ozone and secondary organic aerosol. Chem. Rev. 113, 5848–5870.
Pfeffer, M A, Bergsson, B, Barsotti, S, Stefansdottir, G, Galle, B, Arellano, S, et al., 2018. Ground-based measurements of the 2014-2015 Holuhraun volcanic cloud (Iceland). Geosci. Basel 8, 29.
Rodriguez, J.A., Jirsak, T., Liu, G., Hrbek, J., Dvorak, J., Maiti, A., 2001. Chemistry of NO_2 on oxide surfaces: formation of NO_3 on TiO_2(110) and $NO_2 \leftrightarrow O$ vacancy interactions. J. Am. Chem. Soc. 123, 9597–9605.
Romanias, M.N., Bedjanian, Y., Zaras, A.M., Andrade-Eiroa, A., Shahla, R., Dagaut, P., et al., 2013. Mineral oxides change the atmospheric reactivity of soot: NO_2 uptake under dark and UV irradiation conditions. J. Phys. Chem. A 117, 12897–12911.
Romanias, M.N., El Zein, A., Bedjanian, Y., 2012. Heterogeneous interaction of H_2O_2 with TiO_2 surface under dark and UV light irradiation conditions. J. Phys. Chem. A 116, 8191–8200.
Romanias, M.N., Zeineddine, M.N., Gaudion, V., Lun, X., Thevenet, F., Riffault, V., 2016. Heterogeneous interaction of isopropanol with natural Gobi dust. Environ. Sci. Technol. 50, 11714–11722.
Romanías, M.N., Ourrad, H., Thévenet, F., Riffault, V., 2016. Investigating the heterogeneous interaction of VOCs with natural atmospheric particles: adsorption of limonene and toluene on Saharan mineral dusts. J. Phys. Chem. A 120, 1197–1212.
Romanias, M.N., Zeineddine, M.N., Riffault, V., Thevenet, F., 2017. Isoprene heterogeneous uptake and reactivity on TiO_2: a kinetic and product study. Int. J. Chem. Kinet. 49, 773–788.
Romer, P.S., Wooldridge, P.J., Crounse, J.D., Kim, M.J., Wennberg, P.O., Dibb, J.E., et al., 2018. Constraints on aerosol nitrate photolysis as a potential source of HONO and NOx. Environ. Sci. Technol. 52, 13738–13746.
Schneider, J., Matsuoka, M., Takeuchi, M., Zhang, J., Horiuchi, Y., Anpo, M., et al., 2014. Understanding TiO_2 photocatalysis: mechanisms and materials. Chem. Rev. 114, 9919–9986.
Tang, M., Cziczo, D.J., Grassian, V.H., 2016. Interactions of sater with mineral dust aerosol: water adsorption, hygroscopicity, cloud condensation, and ice nucleation. Chem. Rev. 116, 4205–4259.
Tang, M.J., Cox, R.A., Kalberer, M., 2014. Compilation and evaluation of gas phase diffusion coefficients of reactive trace gases in the atmosphere: volume 1. Inorganic compounds. Atmos. Chem. Phys. 14, 9233–9247.
Tang, M.J., Huang, X., Lu, K.D., Ge, M.F., Li, Y.J., Cheng, P., et al., 2017. Heterogeneous reactions of mineral dust aerosol: implications for tropospheric oxidation capacity. Atmos. Chem. Phys. 17, 11727–11777.
Thorsteinsson, T., Gísladóttir, G., Bullard, J., McTainsh, G., 2011. Dust storm contributions to airborne particulate matter in Reykjavík, Iceland. Atmos. Environ. 45, 5924–5933.
Topaloglou, C., Kazadzis, S., Bais, A.F., Blumthaler, M., Schallhart, B., Balis, D., 2005. NO_2 and HCHO photolysis frequencies from irradiance measurements in Thessaloniki, Greece. Atmos. Chem. Phys. 5, 1645–1653.
Urupina, D., Lasne, J., Romanias, M.N., Thiery, V., Dagsson-Waldhauserova, P., Thevenet, F., 2019. Uptake and surface chemistry of SO_2 on natural volcanic dusts. Atmos. Environ. 217, 116942.
Vignelles, D., Roberts, T.J., Carboni, E., Ilyinskaya, E., Pfeffer, M., Dagsson Waldhauserova, P., et al., 2016. Balloon-borne measurement of the aerosol size distribution from an Icelandic flood basalt eruption. Earth Planet. Sci. Lett. 453, 252–259.
von Schneidemesser, E., Monks, P.S., Allan, J.D., Bruhwiler, L., Forster, P., Fowler, D., et al., 2015. Chemistry and the linkages between air quality and climate change. Chem. Rev. 115, 3856–3897.
Wilson, T.M., Cole, J.W., Stewart, C., Cronin, S.J., Johnston, D.M., 2011. Ash storms: impacts of wind-remobilised volcanic ash on rural communities and agriculture following the 1991 Hudson eruption, southern Patagonia, Chile. Bull. Volcanol. 73, 223–239.
Zein, A.E., Romanias, M.N., Bedjanian, Y., 2014. Heterogeneous interaction of H_2O_2 with Arizona test dust. J. Phys. Chem. A 118, 441–448.
Zeineddine, M.N., Romanias, M.N., Gaudion, V., Riffault, V., Thevenet, F., 2017. Heterogeneous interaction of isoprene with natural Gobi dust. ACS Earth Space Chem. 1, 236–243.